DYNALIGN: UNSUPERVISED DYNAMIC TAXONOMY ALIGNMENT FOR CROSS-DOMAIN SEGMENTATION

Anonymous authors
Paper under double-blind review

ABSTRACT

Current unsupervised domain adaptation (UDA) methods for semantic segmentation typically assume identical class labels between the source and target domains. This assumption ignores the label-level domain gap, which is common in real-world scenarios, thus limiting their ability to identify finer-grained or novel categories without requiring extensive manual annotation. A promising direction to address this limitation lies in recent advancements in foundation models, which exhibit strong generalization abilities due to their rich prior knowledge. However, these models often struggle with domain-specific nuances and under-represented fine-grained categories. To address these challenges, we introduce DynAlign , a framework that integrates UDA with foundation models to bridge both the image-level and label-level domain gaps. Our approach leverages prior semantic knowledge to align source categories with target categories that can be novel, more fine-grained, or named differently (e.g., *'vehicle'* to {*'car'*, *'truck'*, *'bus'*}). Foundation models are then employed for precise segmentation and category reassignment. To further enhance accuracy, we propose a knowledge fusion approach that dynamically adapts to varying scene contexts. DynAlign generates accurate predictions in a new target label space without requiring any manual annotations, allowing seamless adaptation to new taxonomies through either model retraining or direct inference. Experiments on the street scene semantic segmentation benchmarks GTA→Mapillary Vistas and GTA→IDD validate the effectiveness of our approach, achieving a significant improvement over existing methods. Our code will be publically available.

1 INTRODUCTION

Semantic segmentation is a crucial computer vision task that assigns category labels to each pixel in an image, enabling detailed scene understanding. Driven by advancements in deep learning, the field has recently seen significant progress, with applications ranging from autonomous driving (Cheng et al., 2022; Jain et al., 2023) to medical image diagnosis (Cao et al., 2022). Despite this progress, models trained on labeled source datasets often struggle to generalize to data with different distributions due to variations in weather, illumination, or object appearance, resulting in degraded performance. While re-training or fine-tuning models can address this issue, these approaches require annotated in-domain data, which is particularly costly for semantic segmentation.

Unsupervised Domain Adaptation (UDA) addresses the challenge of adapting a model trained on a labeled source domain to an unlabeled target domain by mitigating the adverse effects of domain shift without requiring costly data annotations. However, most UDA are constrained by domain-specific knowledge from the available datasets and typically operate under closed-set assumptions, where the label spaces of the two domains are identical. This assumption limits their applicability in real-world scenarios, where source and target datasets often exhibit the label-level taxonomy gap - including variations in class categories, semantic contexts, and category granularity.

To overcome this limitation, open-set Domain Adaptation (DA) methods have been developed to recognize novel classes in the target domain (Saito & Saenko, 2021; Li et al., 2023). However, these methods are only capable of distinguishing *unknown* classes from *known* ones and do not provide detailed classifications for new target classes. To solve this, taxonomy-adaptive domain adaptation has been proposed, enabling UDA in settings where the target domain adopts a label space

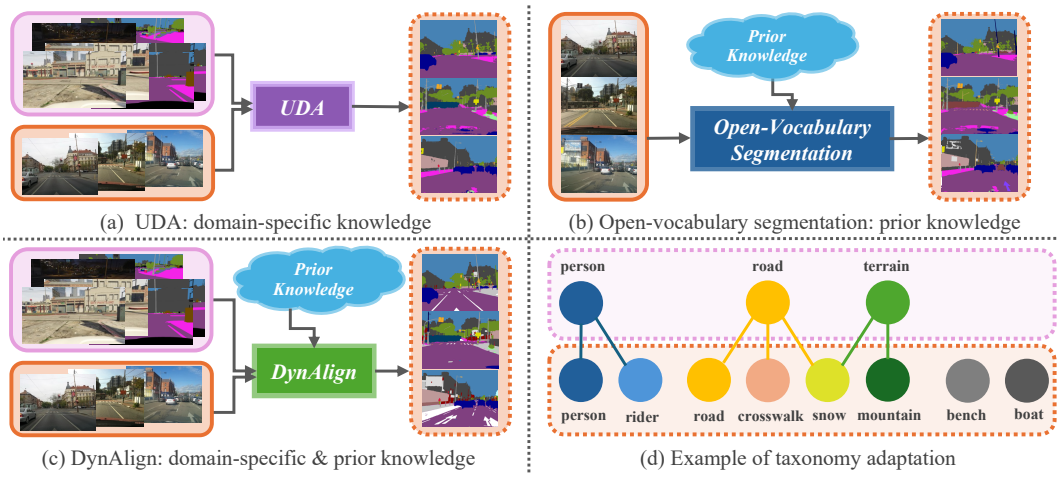

(a) UDA: domain-specific knowledge (b) Open-vocabulary segmentation: prior knowledge

(c) DynAlign: domain-specific & prior knowledge (d) Example of taxonomy adaptation

Figure 1: **DynAlign and taxonomy adaptation.** Current UDA methods focus solely on domain-specific knowledge transfer and assume consistent class labels across domains, limiting their flexibility in adapting to different taxonomies. Open-vocabulary segmentation models excel with broader taxonomies through large-scale pretraining but lack the precision of domain-specific models for specialized tasks. In contrast, DynAlign integrates with any UDA model and flexibly adapts to diverse taxonomies and scene contexts, leveraging the prior knowledge of foundational models.

different from that of the source domain (Gong et al., 2022; Fan et al., 2023a). These methods aim to align differing taxonomies by leveraging relationships between source and target classes but still require prior knowledge about the target labels through annotated samples from the target domain. These challenges highlight the need for a more flexible approach that can simultaneously manage domain shifts while accommodating new taxonomies *without requiring additional annotations from the target domain*. Despite the significance of this problem, fully unsupervised methods that can address both domain shifts and taxonomy discrepancies remain largely underexplored.

Recent advancements in foundation models offer a promising direction to overcome these limitations. By leveraging large-scale pretraining on diverse datasets, these models can generalize across varied domains, tackling the challenges posed by limited domain knowledge and unseen categories. For instance, recent open-vocabulary semantic segmentation works (Ghiasi et al., 2022; **?**) leverage the knowledge in foundation models like CLIP (Radford et al., 2021) and Segment Anything (SAM) (Kirillov et al., 2023), enabling segmentation across a broad range of unbounded class labels. However, despite their strong generalization ability, foundation models often struggle with inferior performance compared to domain-specific models trained on in-domain datasets. Their broad focus can limit their effectiveness in specialized tasks, such as street scene understanding, where fine-grained segmentation requires detailed, domain-specific knowledge.

To conclude, existing works have been tackling image-level and label-level domain gaps separately, while the intersection of these two problems remains underexplored. In this work, we propose a new benchmark of unsupervised taxonomy adaptation, addressing both image-level and label-level domain gaps without supervision, as shown in Figure 1 (c). To achieve this, we propose DynAlign , a novel approach that integrates both domain-specific knowledge and rich open-world prior knowledge from foundation models. The framework first leverages domain-specific knowledge by aligning the data distributions of the source and target domains within the UDA paradigm. Subsequently, to incorporate prior knowledge from foundation models, DynAlign dynamically adapts to new scene contexts by retrieving in-domain predictions and extending the knowledge with foundation models to generate predictions in the new target label space, accommodating the different taxonomy in the target domain. In DynAlign , foundational model knowledge is fused in three modules. First, Large Language Model (LLM) is used for semantic taxonomy mapping and context-aware descriptions. For instance, the source domain label *'road'* is mapped to {*'road'*, *'sidewalk'*, *'lane marking'*, *etc.*} in the target domain, and then each label such as *'lane marking'* can be further enriched with more precise descriptions like {*'traffic lane marking'*, *'double lines'*} to capture the current context and improve semantic granularity. Then, SAM is employed to refine the coarse semantic masks generated by the UDA model, providing more fine-grained masks within precise boundaries (e.g., segmenting *'lane marking'*, *'catch basin'* within the *'road'* region). Lastly, a knowledge fusion mech-

anism is introduced, where CLIP is leveraged to extract textual features based on the context-aware taxonomy provided by LLM and reassign semantic labels to the proposed mask regions, effectively fusing UDA knowledge with prior knowledge. Predictions from DynAlign can be directly used or leveraged as pseudo-labels to train an offline segmentation model on the target domain, enabling instant inference without the need for target domain annotations.

Our approach operates in a fully unsupervised manner, integrating seamlessly with any UDA-based semantic segmentation model. By leveraging the prior knowledge of foundation models, it strengthens in-domain predictions and flexibly adapts to new classes and scene contexts. When the target label set changes, only the taxonomy mapping needs to be updated to instantly predict on the target dataset without requiring additional training. This adaptability offers a highly flexible solution for cross-domain semantic segmentation in dynamic, real-world environments with changing taxonomies. We conduct extensive experiments on the GTA→ Mapillary Vistas and GTA → IDD street scene semantic segmentation benchmarks. The results demonstrate that our method effectively combines domain-specific knowledge with prior knowledge from foundation models, achieving superior performance in the unsupervised taxonomy-adaptive domain adaptation task.

2 Related Works

2.1 Unsupervised Domain Adaptation

Unsupervised domain adaptation (UDA) aims to minimize the domain gap and transfer knowledge from a labeled source domain to an unlabeled target domain. Due to the ubiquity of domain gaps, UDA methods have been widely applied to major computer vision problems including image and video classification (Zhang et al., 2023; Lai et al., 2023; Zara et al., 2023), object detection (Chen et al., 2018; Li et al., 2022b;c; Fan et al., 2023b), and semantic segmentation (Tsai et al., 2018; Hoyer et al., 2022a; 2023). UDA approaches typically minimize domain gaps through methods like discrepancy minimization (Long et al., 2015), adversarial training (Ganin et al., 2016; Long et al., 2018; Shi & Liu, 2024), self-training (Pan et al., 2019; Mei et al., 2020; Zhang et al., 2021). Recently, foundation models have been used to further enhance the adaptation performance by leveraging large-scale pretraining (Fahes et al., 2023; Tang et al., 2024; Gondal et al., 2024).

While traditional UDA methods assume a consistent label space between the source and target domains , this assumption is often violated in real-world scenarios. To address this, several specialized UDA methods have been developed to handle different label shift scenarios (Tachet des Combes et al., 2020; Garg et al., 2023; Westfechtel et al., 2023). Partial DA (Cao et al., 2018; Guo et al., 2022) addresses situations where the target domain contains a subset of the source domain's classes. Open-set DA (Saito & Saenko, 2021; Li et al., 2023) handles cases where the target domain includes unknown classes not present in the source domain. Universal DA (You et al., 2019; Qu et al., 2024) aims to adapt to target domains with any combination of known and unknown classes.

Typically, In the field of cross-domain semantic segmentation, various UDA approaches have been proposed to address the challenges posed by the fine-grained task. Class-incremental DA (Kundu et al., 2020) focuses on adding new classes while preserving knowledge of previously learned ones. Open-set adaptation methods (Bucher et al., 2021; Choe et al., 2024) aim to predict the boundaries of unknown classes. However, these works can only distinguish between the unknown classes and the known ones and do not perform further classification on the unknown classes. Taxonomy adaptive DA (Gong et al., 2022; Fan et al., 2023a) utilizes a more flexible taxonomy mapping where the target label space differs from the source domain. Despite being able to distinguish novel target classes further, these methods cannot be applied in a fully unsupervised DA setting as they rely on few-shot labeled samples from the target domain to gain knowledge on novel classes. Instead, DynAlign leverage prior knowledge from foundation models for unsupervised adaptation.

2.2 Open-vocabulary Semantic Segmentation

Open-vocabulary semantic segmentation aims to assign a semantic label to each pixel of an image using an arbitrary open-vocabulary label set (Xian et al., 2019; Bucher et al., 2019). Recent advancements in vision-language models like CLIP (Radford et al., 2021) have enabled zero-shot classification with enhanced generalization ability from large-scale pretraining, leading to their wide application in open-vocabulary tasks, including semantic segmentation (Li et al., 2022a).

To adapt CLIP for better performance in dense prediction tasks, different approaches have been explored, including fine-tuning CLIP (Liang et al., 2023; Cho et al., 2024) and modifying CLIP's model architecture (Wang et al., 2023; Yu et al., 2024). For finer segmentation boundaries, two-stage frameworks involving mask proposal generation followed by classification remain prominent in open-vocabulary semantic segmentation (Kirillov et al., 2023; Wu et al., 2023a; Ding et al., 2022). The recent advent of Segment Anything Model (SAM) (Kirillov et al., 2023) provides a free and precise mask proposal generation approach and thus integrated by several works to enhance the performance (Shi & Yang, 2024; Li et al., 2024; Yuan et al., 2024). Despite these advancements, open-vocabulary methods struggle with domain-specific nuances and fine-grained categories (Zhou & Beyerer, 2023; Wu et al., 2023b). Wei et al. (2024) leverages vision foundation models to improve the generalization ability of task-specific semantic segmentation models. Yilmaz et al. (2024) incorporates domain-specific knowledge into the open-vocabulary framework through supervised prompt fine-tuning, whereas our work focuses on fully unsupervised adaptation.

3 Problem Definition

We formulate the problem of unsupervised taxonomy adaptive cross-domain semantic segmentation as follows: given a labeled source domain $\mathcal{D}_s$ with a label set $\mathbb{C}_s$, our goal is to achieve semantic segmentation on an unlabeled target domain $\mathcal{D}_t$ with a known label set $\mathbb{C}_t$. Specifically, we have:

- a labeled source domain $\mathcal{D}_s = \{X_s, Y_s\}$, where $X_s \in \mathbb{R}^{H\times W\times 3}$ represents RGB images and Y_s denotes pixel-wise annotations in the source label set $\mathcal{C}_s = \{c_s^1, c_s^2, \ldots, c_s^m\}$.
- an unlabeled target domain $\mathcal{D}_t = \{X_t\}$. The ground truth pixel-wise annotations belong to the known target label space $\mathbb{C}_t = \{c_t^1, c_t^2, ..., c_t^n\}$ and are not available during training.
- $\mathbb{C}_s$ and $\mathbb{C}_t$ may have inconsistent taxonomies. This inconsistency may involve differences in label granularity, hierarchical class structures (such as subclasses), or the introduction of entirely new categories in $\mathbb{C}_t$, as illustrated in Figure 1 (d).

Formally: Let P_s and P_t represent the distributions of source domain data X_s and target domain data X_t, respectively. In the context of taxonomy-adaptive cross-domain semantic segmentation, three primary challenges need to be addressed:

- Image-level domain gap: the source and target data have distinct data distributions ($P_s \neq P_t$).
- Label-level taxonomy inconsistency: the source and target label sets are different ($\mathbb{C}_s \neq \mathbb{C}_t$).
- Absence of target domain annotations: no labeled data is available for the target domain.

We aim to train a model using both the labeled source domain $\mathcal{D}_s$ and the unlabeled target domain $\mathcal{D}_t$, and evaluate the performance on the target dataset $\mathcal{D}_t$ within the label space $\mathbb{C}_t$.

4 Method

Method Overview In this work, we propose DynAlign, a novel framework for unsupervised taxonomy-adaptive cross-domain semantic segmentation that fuses domain-specific knowledge with text and visual prior knowledge. Our method comprises three main stages: incorporating domain knowledge, incorporating prior knowledge, and combining them through a knowledge fusion mechanism, as illustrated in Figure 2. In the first stage, we integrate domain-specific knowledge by training a domain-specific model on the available labeled source domain and unlabeled target domain, which generates predictions within the source label space (Section 4.1). In the second stage, we incorporate both text & vision prior knowledge to address the label-level taxonomy inconsistency. Specifically, we use LLM to construct a taxonomy mapping to link the source labels with the target labels and further enrich the target labels with context descriptions (see Section 4.2). Then we utilize SAM to generate mask proposals that segment the image into fine-grained semantic regions and extract multi-scale visual information for each region (see Section 4.3). In the final stage, we introduce knowledge fusion mechanism (see Section 4.4), where the domain-specific predictions and prior knowledge are integrated based on CLIP. As shown in Figure 3, for each mask proposal from SAM, we take the majority pixel label of in-domain prediction as the initial source label and retrieve the correlated target classes from the taxonomy mapping. CLIP is then used to extract the multi-scale regional visual features and the context-aware text features for the mapped target classes. Finally, each fine-grained mask region is reclassified based on CLIP feature similarity.

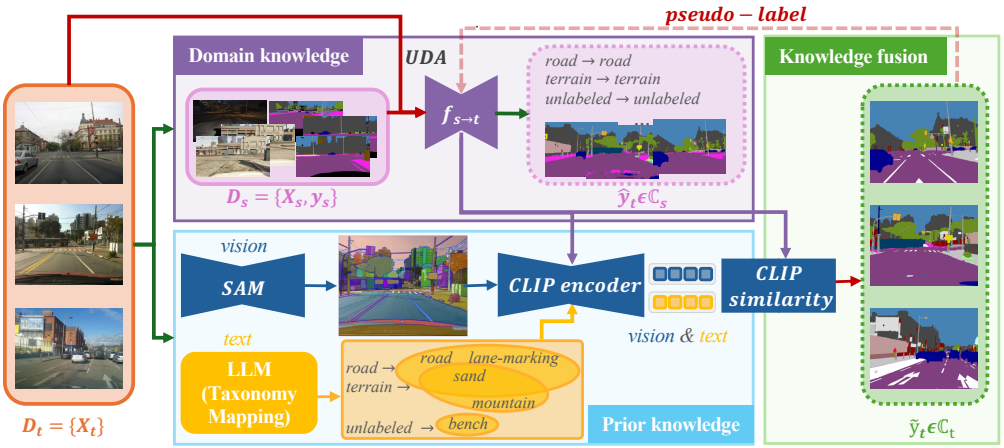

Figure 2: **DynAlign overview.** DynAlign integrates with any UDA model, leveraging its domain-specific knowledge and enhancing it with prior knowledge from foundation models. DynAlign starts with coarse UDA model predictions, followed by: 1) LLM constructing taxonomy mappings to align source and target domains; 2) SAM generating fine-grained masks. CLIP is deployed to fuse the visual knowledge from SAM with the semantic knowledge from LLM to reassign accurate labels. The CLIP-fused predictions can be used as pseudo-labels to further fine-tune the UDA model.

4.1 Domain-specific knowledge

To gain domain-specific knowledge, given a labeled source domain $\mathcal{D}_s$ and an unlabeled target domain $\mathcal{D}_t$, we train a domain-specific model $f_{s\to t}$ by leveraging data from both domains. Specifically, we follow the UDA paradigm, which aligns the data distribution of the source and target domains. This adapted model integrates supervised knowledge from the source domain with visual information from the target domain, enabling it to generate accurate predictions on the unlabeled target dataset $\mathcal{D}_t$ within the source label space $\mathbb{C}_s$.

In our experiments, we develop an UDA model inspired by the architecture proposed by Hoyer et al. (2022b). The model comprises a hierarchical transformer encoder, based on the design of Xie et al. (2021), combined with a multi-scale decoder that effectively integrates contextual information from low-level features. Initially, the model is trained using a supervised cross-entropy loss on the labeled source domain $\mathcal{D}_s$. Then, we adapt it to the unlabeled target domain $\mathcal{D}_t$ through an unsupervised self-training. This adaptation process incorporates a teacher network that generates pseudo-labels for the target domain, which are then weighted based on confidence estimates to account for uncertainty. These weighted pseudo-labels are used to further refine the model's performance on the target domain. The adapted model learns shared feature representations for both domains, enabling it to effectively handle image-level domain shifts. Detailed model architecture and training procedures are provided in the Appendix A.1. We leverage the knowledge learned by $f_{s\to t}$ to generate initial predictions $\hat{y}_t$ for the target images within the source label set $\mathbb{C}_s$.

4.2 Semantic taxonomy mapping

The acquired domain-specific model is constrained by the in-domain knowledge, thus limiting their ability to generalize beyond the learned source label space to a new target label space. To bridge this gap, we introduce a taxonomy reasoning process that adapts the label space from $\mathbb{C}_s$ to $\mathbb{C}_t$. This taxonomy mapping enables the model to semantically link source domain labels to the known target domain label set $\mathbb{C}_t$. For instance, the source label *'road'* can be mapped to more granular target domain labels such as {*'road', 'sidewalk', 'curb', 'lane marking', 'rail track', etc.*}. We construct a taxonomy mapping for each source label to connect the source and target label spaces. This mapping is flexibly defined, allowing for differences in label granularity, hierarchical class structures (such as subclasses), or the introduction of entirely new categories, as shown in Figure 1 (d).

Formally, given the source domain label set $\mathbb{C}_s = \{c_s^1, c_s^2, \ldots, c_s^m\}$ and the target domain label set $\mathbb{C}_t = \{c_t^1, c_t^2, ..., c_t^n\}$, we define the taxonomy mapping for each source domain label c_s^i as:

$$c_s^i \to \mathbb{C}_t^i \subseteq \mathbb{C}_t, \quad 1 \leq i \leq m \tag{1}$$

where $\mathbb{C}_t^i$ represents an arbitrary subset of $\mathbb{C}_t$ that semantically correlates with the source domain label c_s^i. For novel classes that are not present in the source domain, we map them to each source label, enabling better discovery of these new classes. Further details about the taxonomy mapping can be found in the Appendix A.7.

To extract meaningful semantic features, we use the CLIP text encoder to encode text features for each target label. Original class labels often lack sufficient context and semantic richness, leading to ambiguity and imprecision. For example, the label *'bridge'* in street scene segmentation datasets is too generic and might be interpreted as a bridge over a river rather than a pedestrian bridge in urban environments. This lack of specificity can cause confusion and misclassification in the segmentation process, resulting in inferior performance. To address this, we enhance the semantic clarity of each target class label by expanding it with contextually relevant synonyms or related phrases. For each target class label, we use GPT-4 (Achiam et al., 2023) to generate a set of contextually relevant terms, such as *'bridge'* $\rightarrow$ {*'road bridge', 'footbridge', 'pedestrian bridge', etc.*}. These terms are generated by prompting GPT-4 with descriptions of the dataset context and the original class label. More details are provided in the appendix A.8. This additional contextual information helps reduce ambiguity and improve the accuracy of mask region classification. We then compute the **context-aware text feature** for each target domain label. Specifically, for each target domain label $c_t^j \in \mathbb{C}_t$, we generate a context description set $\mathbb{C}_{context}^j$ and compute the CLIP encoded text feature for each description $c_{context} \in \mathbb{C}_{context}^j$. The text feature for class label c_t^j is then obtained by averaging all the contextual description features, as follows:

$$F_t^j = \text{average}\, \Phi^T(c_{context}), \quad c_{context} \in \mathbb{C}_{context}^j \tag{2}$$

where $\Phi^T(\cdot)$ represents CLIP text encoder. We then aggregate these features to form the final text feature representations of the target domain label space denoted as $\mathbb{F}_{target} = \{F_t^1, F_t^2, ..., F_t^n\}$. For each source label c_s^i, we retrieve its mapped target labels $\mathbb{C}_t^i$ and the corresponding feature representation set $\mathbb{F}_T^i \subseteq \mathbb{F}_{target}$ as the semantic representation.

4.3 Visual prior knowledge

To identify new labels in the target domain, it is essential to align visual information with the target domain label set and its novel semantic categories. Therefore, we incorporate prior knowledge from general-purpose foundation models to enhance visual understanding. We first generate mask proposals using the Segment-Anything-Model (SAM) (Kirillov et al., 2023), which is renowned for its zero-shot capability to produce high-quality, fine-grained masks with precise segmentation boundaries. With SAM, we are able to obtain a set of mask regions that likely correspond to semantically meaningful object boundaries.

Next, we capture semantic visual information for each mask region by extracting visual embeddings using CLIP, which requires capturing both fine-grained details and broader contextual information. To obtain more representative features, we propose **multi-scale visual feature extraction**, which concatenates local and multi-scale global features. Given a target domain image x_t, and a binary mask proposal m from SAM, we obtain the masked local region $r = x_t \odot m$ and a bounding box b that crops the masked region. The local feature is extracted with CLIP vision encoder $\Phi^V(\cdot)$, as:

$$F_l = \Phi^V(b) \tag{3}$$

Specifically, we use ConvCLIP (Yu et al., 2024) vision encoder due to its advantage in dense prediction tasks. To capture broader contextual information, we incorporate global features by averaging embeddings across multiple scales. This is achieved by adding multi-scale padding around each local bounding box region b, as illustrated in Figure 3. The padding size is adjusted based on the class labels, with larger objects like *'road'* assigned larger padding sizes, and smaller objects like *'bicycle'* assigned smaller padding sizes. For each bounding box b, we create a set of padded global regions $\mathbb{B}$ and extract the corresponding global feature:

$$\mathbb{F}_g = \{\Phi^V(b_k)\}, \quad b_k \in \mathbb{B} \tag{4}$$

To combine both local and global visual information, we extract the final visual feature F_V as the weighted sum of $\mathbb{F}_g$ and F_l. Specifically, we calculate the cosine similarity between the local feature

F_l and each global feature $F_{g_k} \in \mathbb{F}_g$. The similarity scores ϕ_k are computed as follows:

$$\phi_k = \langle F_l, F_{g_k} \rangle = \frac{(F_l)^T F_{g_k}}{\|F_l\| \, \|F_{g_k}\| + \epsilon}, \quad F_{g_k} \in \mathbb{F}_g. \tag{5}$$

where ϵ is a small constant. Subsequently, we derive the final multi-scale visual feature F_V for the current mask region by aggregating the local feature F_l with the global features F_g, weighted by their respective cosine similarities ϕ_k. This aggregation ensures that both local details and broader contextual information contribute effectively to the visual feature representation:

$$F_V = \frac{\Sigma(\phi_k F_{g_k} + (1 - \phi_k) F_l)}{|\mathbb{F}_g|}, \quad F_{g_k} \in \mathbb{F}_g. \tag{6}$$

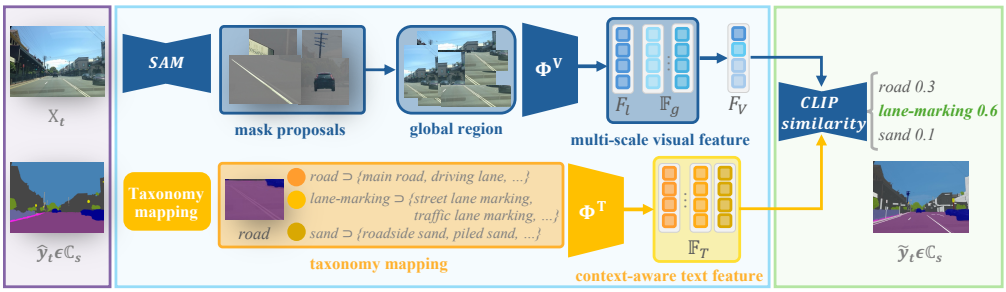

Figure 3: **Foundational models and knowledge fusion.** The fine-grained mask proposals from SAM are encoded into multi-scale visual features using CLIP's vision encoder, while the enriched target domain taxonomies from LLM are encoded as context-aware text features via CLIP's text encoder. The similarity between these visual and text embeddings is then calculated to reassign semantic taxonomies accurately to the fine-grained masks in the target domain. Here, $\Phi^V(\cdot)$ and $\Phi^T(\cdot)$ denote the CLIP vision and text encoders, respectively. F_l and $\mathbb{F}_g$ represent the local and global features, while F_V denotes their weighted sum, forming the final extracted multi-scale visual feature to represent the mask region. $\mathbb{F}_T$ refers to the extracted text feature set of candidate classes.

4.4 Knowledge Fusion

Given the domain-specific knowledge and prior knowledge from foundation models, we aim to fuse them to bridge both image-level and label-level domain gaps. The general fusion process of DynAlign is shown in Figure 3.

Given a target image x_t, we generate mask proposals that segment the image into fine-grained regions using SAM. For each mask region m, we first associate it with the source domain label space by retrieving in-domain knowledge from the label prediction $\hat{y}_t$ generated by model $f_{s \to t}$ (as described in Section 4.1) The initial label c_s^i for mask region m is determined by the majority of predicted pixel labels within that mask area. To reassign each mask region with new target labels, given the source label c_s^i, we retrieve its related target domain label subsets $c_s^i \to \mathbb{C}_t^i \subseteq \mathbb{C}_t$ and the corresponding feature representation set $\mathbb{F}_T \subseteq \mathbb{F}_{target}$ using prior knowledge from the taxonomy mapping (see Section 4.2). Additionally, based on the initial label c_s^i, we adjust the appropriate padding size of the global region $\mathbb{B}$ (see Section 4.3) accordingly to enrich the visual context and extract the multi-scale visual feature F_V, serving as the regional visual feature representation. Finally, each mask region is reassigned a new target label based on the largest similarity between the context-aware text features $\mathbb{F}_T$ and multi-scale visual feature F_V as:

$$\phi = \langle F_V, \mathbb{F}_T \rangle, \quad \tilde{y}_t = \text{argmax}(\phi) \tag{7}$$

We reassign the label of each mask region from $\hat{y}_s$ to the newly estimated $\tilde{y}_t$ when the confidence exceeds 0.5. This reassignment is applied to every mask proposal within the image sample x_t, thereby updating the pixel-wise semantic pseudo-labels in the target domain.

DynAlign generates predictions for new classes in the target domain that were not present in the source domain, eliminating the need for manual annotations. This capability allows the model to

adapt flexibly to new target classes and when the target label set changes, we simply redefine the taxonomy mapping to generate new predictions for the target domain dataset. This two-step process– mapping known classes and discovering new ones – enables our framework to effectively adapt to the target domain's taxonomy in a fully unsupervised manner.

5 EXPERIMENT

5.1 IMPLEMENTATION DETAILS

Datasets We evaluate our method using the synthetic dataset GTA as the source domain and two real-world datasets, Mapillary Vistas and India Driving Dataset (IDD), as target domains. **GTA** (Richter et al., 2016) is a synthetic dataset with pixel-level annotations for 19 semantic classes. It serves as the labeled source domain in our experiments. **Mapillary Vistas** (Neuhold et al., 2017) contains 25k high-resolution images collected from a wide variety of environments, weather conditions, and geographical locations. It is annotated with 66 object categories, providing a highly challenging real-world target domain. **IDD** dataset (Varma et al., 2019), captured from Indian urban driving scenes, is characterized by complex and varied road environments. It contains 10,003 images annotated with 25 semantic classes at level 3 granularity. For evaluation, we focus on 45 classes from Mapillary Vistas and 24 from IDD, excluding small-scale or less informative categories.

Experimental setup For the unsupervised taxonomy-adaptive domain adaptation task, we use the GTA training set as the labeled source domain and the training sets of Mapillary Vistas and IDD as the unlabeled target domains. No target domain annotations are used during training, ensuring a fully unsupervised domain adaptation setup. We perform image-level adaptation by training the model $f_{s\to t}$ on the labeled source domain and each of the unlabeled target domains separately, following the default training parameters in Hoyer et al. (2022b). For label-level adaptation, we define a taxonomy mapping between the source and target labels (see Appendix A.7) and context descriptions for target labels (see Appendix A.8). Performance is reported on the validation set of each target dataset. We employ the ViT-L SAM model (**?**) and the ConvNeXt-Large CLIP model (Yu et al., 2024) by default. More experimental details are provided in the appendix A.1.

Evaluation metrics We evaluate the performance using two standard semantic segmentation metrics. Mean Intersection over Union (mIoU) calculates the average intersection over union for each class and then averages across all classes. Mean Accuracy (mAcc) calculates the percentage of correctly predicted pixels for each class and then averages the results across all classes.

5.2 EXPERIMENTAL RESULTS

To the best of our knowledge, our work is the first to investigate the fully unsupervised taxonomy-adaptive domain adaptation problem. Traditional DA methods are limited to fixed label spaces, making them inapplicable to our problem setting. Therefore, we compare our proposed method, DynAlign , with open-vocabulary segmentation methods, Grounded-SAM (Ren et al., 2024) and OWL-VIT (Matthias Minderer, 2023). Additionally, we evaluate the naive combination of these methods with HRDA, where HRDA generates predictions for classes matching the source labels, while open-vocabulary methods are employed to predict new classes (see Appendix A.3 for more illustration). The comparative results are summarized in Table 1.

Table 1: Open-vocabulary semantic segmentation comparisons on Mapillary Vistas and IDD

Methods	Mapillary Vistas						IDD					
	all		known		unknown		all		known		unknown	
	mACC	mIoU	mACC	mIoU	mACC	mIoU	mACC	mIoU	mACC	mIoU	mACC	mIoU
Grounded-SAM	33.1	28.6	46.7	43.0	24.0	18.3	36.0	30.8	43.7	37.2	16.1	14.1
OwlVIT-SAM	29.6	19.5	32.7	26.7	27.5	14.7	31.6	20.9	33.3	23.1	27.3	15.2
HRDA	-	-	75.8	65.8	-	-	-	-	68.9	61.3	-	-
HRDA + Grounded-SAM	40.4	32.9	63.6	53.1	25.0	19.4	51.7	39.4	65.6	49.3	16.1	14.1
HRDA + OwlVIT-SAM	40.2	28.8	56.1	48.4	29.5	15.6	55.9	40.2	**67.1**	49.9	27.3	15.2
Ours	**53.0**	**36.7**	**72.6**	**62.4**	**39.9**	**19.6**	**57.7**	**41.7**	66.8	**50.9**	**34.3**	**18.1**

On the Mapillary dataset, open-vocabulary methods, which relies solely on foundation models, demonstrate limited performance. By integrating domain-specific knowledge through HRDA,

the performance improves, with HRDA + Grounded-SAM reaching 32.9% and HRDA + OWL-ViT-SAM achieving 28.8% mIoU. Notably, our method, DynAlign , significantly outperforms all baselines, achieving the highest mIoU of 36.7%. Results on IDD show consistent trends. Open-vocabulary methods alone perform modestly with mIoUs of 30.8% for Grounded-SAM and 20.9% for OWL-ViT-SAM. When combined with HRDA, performance improves to 39.4% and 40.2%, respectively. DynAlign demonstrates again superior performance with the highest mIoU of 41.7%. Notably, for unknown classes, DynAlign achieves an mIoU of 18.1%, surpassing HRDA + Grounded-SAM at 14.1% and HRDA + OWL-ViT-SAM at 15.2%, showing a substantial improvement in accurately segmenting unseen categories. The results demonstrate that incorporating domain-specific knowledge through UDA significantly enhances performance, even when leveraging strong foundation models for open-vocabulary tasks. DynAlign not only preserves the domain knowledge from the UDA baseline but also retains the flexibility to accommodate new classes. This highlights its advantages in effectively integrating both domain knowledge and prior knowledge, highlighting its advantage over traditional UDA methods and open-vocabulary approaches.

We present qualitative comparison results on the Mapillary Vistas dataset in Figure 5. The key new classes are highlighted under each set of results. Our method clearly outperforms the baselines by producing more precise boundaries, better detection of new classes, and more accurate predictions.

5.3 Pseudo-label Training for Segmentation Model

While DynAlign demonstrated superior performance over baseline open-vocabulary methods during inference, we also explored its capability to generate pseudo-labels for training a new segmentation model on the target domain's taxonomy. This approach aims to reduce inference time and potentially boost segmentation accuracy. By generating pseudo-labels on the Mapillary Vistas training set using DynAlign , we train a semantic segmentation model in the new label space (details provided in Appendix A.1). Figure 4 compares direct inference using DynAlign and performance of the trained segmentation model on the validation set. The pseudo-label trained model outperforms direct inference, with mACC improving from 53.0% to 56.2% and mIoU from 36.7% to 38.9%. These results suggest that DynAlign can generate high-quality pseudo-labels, enabling the training of segmentation models that can greatly boost the efficiency and maintain improved performance on the target domain. We report the memory usage and computational efficiency of DynAlign in both direct inference and pseudo-labeling in the appendix A.2.

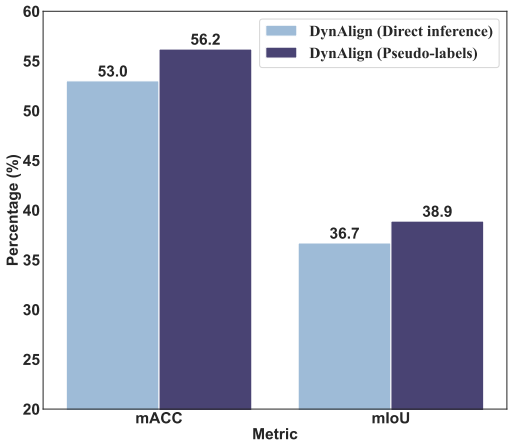

Figure 4: Performance comparison between direct inference and pseudo-label training using DynAlign on the Mapillary Vistas dataset.

Table 2: Ablations on multi-scale visual feature and context-aware text feature

Modules		Mapillary Vistas		IDD	
MS (vision)	CA (text)	mACC	mIoU	mACC	mIoU
✗	✗	44.0	29.0	52.9	37.9
✗	✓	45.4	29.4	52.5	38.0
✓	✗	50.2	35.6	57.0	39.9
✓	✓	**53.0**	**36.7**	**57.7**	**41.7**

Table 3: Ablations on CLIP vision encoders

model	Mapillary Vistas		IDD	
	mACC	mIoU	mACC	mIoU
CLIP	50.8	35.0	54.7	38.0
MaskCLIP	50.5	34.7	54.1	37.5
SCLIP	50.9	36.0	56.8	39.4
ConvCLIP	**53.0**	**36.7**	**57.7**	**41.7**

5.4 Ablation Studies

Multi-scale visual feature & context-aware text feature ablation In contrast to the basic CLIP features, we enhance feature representations by introducing **context-aware text feature (CA-Text)** and **multi-scale visual feature (MS-vision)**. As shown in Table 2, these two strategies have distinct impacts on the performance. Incorporating multi-scale visual features improves the Mapillary mIoU

from 29.0% to 35.6% and the IDD mIoU from 37.9% to 39.9%. The context-aware text feature shows modest gains, particularly on Mapillary, where mIoU rises from 29.0% to 29.4%. Combining both components yields the best results (Mapillary mIoU: 36.7%, IDD mIoU: 41.7%).

DynAlign modules. Table 3 compares the performance of various CLIP backbones in DynAlign framework. ConvCLIP (Yu et al., 2024), the only convolution-based model, outperforms ViT-based models including CLIP (Radford et al., 2021), MaskCLIP (Dong et al., 2023), and SCLIP (Wang et al., 2023), and achieves the best results, with a Mapillary Vistas mIoU of 36.7% and an IDD mIoU of 41.7%. The result shows its advantage in dense prediction tasks when input sizes scale up.

Table 4 shows shows the performance on the Mapillary Vistas dataset when replacing corresponding modules in DynAlign with MIC (Hoyer et al., 2023), MobileSAM (Zhang et al.), and Llama (Touvron et al., 2023). The results demonstrate consistently strong performance across various model integrations, emphasizing DynAlign 's flexibility in seamlessly incorporating foundation models into domain-specific tasks.

Table 4: Ablations on DynAlign modules

Method	mIoU	mAcc
HRDA → MIC	37.7	54.4
SAM → MobileSAM	35.2	51.5
GPT-4 → Llama	37.5	52.1
DynAlign (Ours)	36.7	53.0

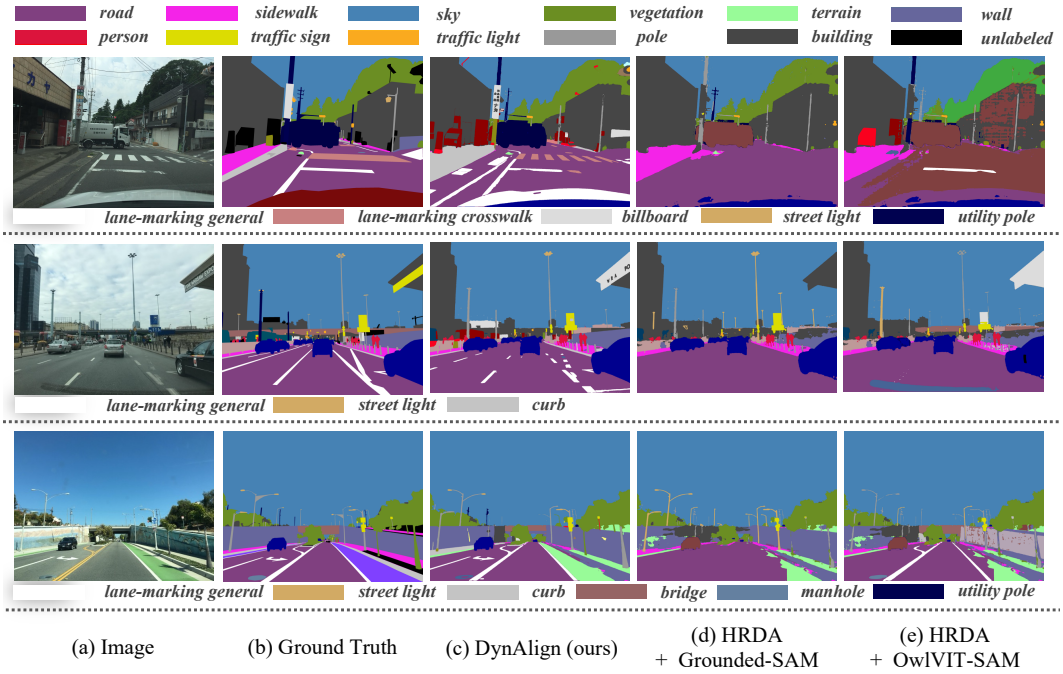

(a) Image (b) Ground Truth (c) DynAlign (ours) (d) HRDA + Grounded-SAM (e) HRDA + OwlVIT-SAM

Figure 5: **Qualitative comparisons on Mapillary Vistas dataset.** DynAlign effectively segments new and fine-grained classes on the target domain, showing strong taxonomy adaptation capabilities.

6 Conclusion

In this paper, we propose DynAlign to address the challenge of unsupervised taxonomy-adaptive cross-domain semantic segmentation, effectively segmenting images across domains with different taxonomies without requiring target domain annotations. DynAlign integrates domain-specific knowledge by utilizing UDA models to bridge the image-level domain gap, and leverages foundation models to resolve label-level taxonomy inconsistencies between domains. The approach demonstrates significant improvements over existing methods on the Mapillary Vistas and IDD street scene datasets, consistently achieving higher mIoU scores for both known and unknown classes.

To the best of our knowledge, we are the first to define and address the unsupervised taxonomy-adaptive domain adaptation problem. Our results demonstrate that DynAlign outperforms not only open-vocabulary segmentation methods but also their naive combinations with domain adaptation techniques. While our research focuses on road scene understanding, the framework has the potential to be extended to other domains with evolving taxonomies.

REFERENCES

Josh Achiam, Steven Adler, Sandhini Agarwal, Lama Ahmad, Ilge Akkaya, Florencia Leoni Aleman, Diogo Almeida, Janko Altenschmidt, Sam Altman, Shyamal Anadkat, et al. Gpt-4 technical report. *arXiv preprint arXiv:2303.08774*, 2023.

Maxime Bucher, Tuan-Hung Vu, Matthieu Cord, and Patrick Pérez. Zero-shot semantic segmentation. *Advances in Neural Information Processing Systems*, 32, 2019.

Maxime Bucher, Tuan-Hung Vu, Matthieu Cord, and Patrick Pérez. Handling new target classes in semantic segmentation with domain adaptation. *Computer Vision and Image Understanding*, 212:103258, 2021.

Hu Cao, Yueyue Wang, Joy Chen, Dongsheng Jiang, Xiaopeng Zhang, Qi Tian, and Manning Wang. Swin-unet: Unet-like pure transformer for medical image segmentation. In *European conference on computer vision*, pp. 205–218. Springer, 2022.

Zhangjie Cao, Mingsheng Long, Jianmin Wang, and Michael I Jordan. Partial transfer learning with selective adversarial networks. In *Proceedings of the IEEE conference on computer vision and pattern recognition*, pp. 2724–2732, 2018.

Yuhua Chen, Wen Li, Christos Sakaridis, Dengxin Dai, and Luc Van Gool. Domain adaptive faster r-cnn for object detection in the wild. In *Proceedings of the IEEE conference on computer vision and pattern recognition*, pp. 3339–3348, 2018.

Bowen Cheng, Ishan Misra, Alexander G Schwing, Alexander Kirillov, and Rohit Girdhar. Masked-attention mask transformer for universal image segmentation. In *Proceedings of the IEEE/CVF conference on computer vision and pattern recognition*, pp. 1290–1299, 2022.

Seokju Cho, Heeseong Shin, Sunghwan Hong, Anurag Arnab, Paul Hongsuck Seo, and Seungryong Kim. Cat-seg: Cost aggregation for open-vocabulary semantic segmentation. In *Proceedings of the IEEE/CVF Conference on Computer Vision and Pattern Recognition*, pp. 4113–4123, 2024.

Seun-An Choe, Ah-Hyung Shin, Keon-Hee Park, Jinwoo Choi, and Gyeong-Moon Park. Open-set domain adaptation for semantic segmentation. In *Proceedings of the IEEE/CVF Conference on Computer Vision and Pattern Recognition*, pp. 23943–23953, 2024.

Zheng Ding, Jieke Wang, and Zhuowen Tu. Open-vocabulary universal image segmentation with maskclip. *arXiv preprint arXiv:2208.08984*, 2022.

Xiaoyi Dong, Jianmin Bao, Yinglin Zheng, Ting Zhang, Dongdong Chen, Hao Yang, Ming Zeng, Weiming Zhang, Lu Yuan, Dong Chen, Fang Wen, and Nenghai Yu. Maskclip: Masked self-distillation advances contrastive language-image pretraining. In *Proceedings of the IEEE/CVF Conference on Computer Vision and Pattern Recognition (CVPR)*, pp. 10995–11005, June 2023.

Mohammad Fahes, Tuan-Hung Vu, Andrei Bursuc, Patrick Pérez, and Raoul De Charette. Poda: Prompt-driven zero-shot domain adaptation. In *Proceedings of the IEEE/CVF International Conference on Computer Vision*, pp. 18623–18633, 2023.

Jianan Fan, Dongnan Liu, Hang Chang, Heng Huang, Mei Chen, and Weidong Cai. Taxonomy adaptive cross-domain adaptation in medical imaging via optimization trajectory distillation. In *Proceedings of the IEEE/CVF International Conference on Computer Vision*, pp. 21174–21184, 2023a.

Qi Fan, Mattia Segu, Yu-Wing Tai, Fisher Yu, Chi-Keung Tang, Bernt Schiele, and Dengxin Dai. Towards robust object detection invariant to real-world domain shifts. In *The Eleventh International Conference on Learning Representations (ICLR 2023)*. OpenReview, 2023b.

Yaroslav Ganin, Evgeniya Ustinova, Hana Ajakan, Pascal Germain, Hugo Larochelle, François Laviolette, Mario March, and Victor Lempitsky. Domain-adversarial training of neural networks. *Journal of machine learning research*, 17(59):1–35, 2016.

Saurabh Garg, Nick Erickson, James Sharpnack, Alex Smola, Sivaraman Balakrishnan, and Zachary Chase Lipton. Rlsbench: Domain adaptation under relaxed label shift. In *International Conference on Machine Learning*, pp. 10879–10928. PMLR, 2023.

Golnaz Ghiasi, Xiuye Gu, Yin Cui, and Tsung-Yi Lin. Scaling open-vocabulary image segmentation with image-level labels. In *European Conference on Computer Vision*, pp. 540–557. Springer, 2022.

Muhammad Waleed Gondal, Jochen Gast, Inigo Alonso Ruiz, Richard Droste, Tommaso Macri, Suren Kumar, and Luitpold Staudigl. Domain aligned clip for few-shot classification. In *Proceedings of the IEEE/CVF Winter Conference on Applications of Computer Vision*, pp. 5721–5730, 2024.

Rui Gong, Martin Danelljan, Dengxin Dai, Danda Pani Paudel, Ajad Chhatkuli, Fisher Yu, and Luc Van Gool. Tacs: Taxonomy adaptive cross-domain semantic segmentation. In *European Conference on Computer Vision*, pp. 19–35. Springer, 2022.

Pengxin Guo, Jinjing Zhu, and Yu Zhang. Selective partial domain adaptation. In *BMVC*, pp. 420, 2022.

Lukas Hoyer, Dengxin Dai, and Luc Van Gool. Daformer: Improving network architectures and training strategies for domain-adaptive semantic segmentation. In *Proceedings of the IEEE/CVF conference on computer vision and pattern recognition*, pp. 9924–9935, 2022a.

Lukas Hoyer, Dengxin Dai, and Luc Van Gool. Hrda: Context-aware high-resolution domain-adaptive semantic segmentation. In *European conference on computer vision*, pp. 372–391. Springer, 2022b.

Lukas Hoyer, Dengxin Dai, Haoran Wang, and Luc Van Gool. Mic: Masked image consistency for context-enhanced domain adaptation. In *Proceedings of the IEEE/CVF conference on computer vision and pattern recognition*, pp. 11721–11732, 2023.

Jitesh Jain, Jiachen Li, Mang Tik Chiu, Ali Hassani, Nikita Orlov, and Humphrey Shi. Oneformer: One transformer to rule universal image segmentation. In *Proceedings of the IEEE/CVF Conference on Computer Vision and Pattern Recognition*, pp. 2989–2998, 2023.

Alexander Kirillov, Eric Mintun, Nikhila Ravi, Hanzi Mao, Chloe Rolland, Laura Gustafson, Tete Xiao, Spencer Whitehead, Alexander C Berg, Wan-Yen Lo, et al. Segment anything. In *Proceedings of the IEEE/CVF International Conference on Computer Vision*, pp. 4015–4026, 2023.

Jogendra Nath Kundu, Rahul Mysore Venkatesh, Naveen Venkat, Ambareesh Revanur, and R Venkatesh Babu. Class-incremental domain adaptation. In *Computer Vision–ECCV 2020: 16th European Conference, Glasgow, UK, August 23–28, 2020, Proceedings, Part XIII 16*, pp. 53–69. Springer, 2020.

Zhengfeng Lai, Noranart Vesdapunt, Ning Zhou, Jun Wu, Cong Phuoc Huynh, Xuelu Li, Kah Kuen Fu, and Chen-Nee Chuah. Padclip: Pseudo-labeling with adaptive debiasing in clip for unsupervised domain adaptation. In *Proceedings of the IEEE/CVF International Conference on Computer Vision*, pp. 16155–16165, 2023.

Boyi Li, Kilian Q Weinberger, Serge Belongie, Vladlen Koltun, and René Ranftl. Language-driven semantic segmentation. *arXiv preprint arXiv:2201.03546*, 2022a.

Wuyang Li, Xinyu Liu, and Yixuan Yuan. Sigma: Semantic-complete graph matching for domain adaptive object detection. In *Proceedings of the IEEE/CVF Conference on Computer Vision and Pattern Recognition*, pp. 5291–5300, 2022b.

Wuyang Li, Jie Liu, Bo Han, and Yixuan Yuan. Adjustment and alignment for unbiased open set domain adaptation. In *Proceedings of the IEEE/CVF Conference on Computer Vision and Pattern Recognition*, pp. 24110–24119, 2023.

Xiangtai Li, Haobo Yuan, Wei Li, Henghui Ding, Size Wu, Wenwei Zhang, Yining Li, Kai Chen, and Chen Change Loy. Omg-seg: Is one model good enough for all segmentation? In *Proceedings of the IEEE/CVF Conference on Computer Vision and Pattern Recognition*, pp. 27948–27959, 2024.

Yu-Jhe Li, Xiaoliang Dai, Chih-Yao Ma, Yen-Cheng Liu, Kan Chen, Bichen Wu, Zijian He, Kris Kitani, and Peter Vajda. Cross-domain adaptive teacher for object detection. In *Proceedings of the IEEE/CVF Conference on Computer Vision and Pattern Recognition*, pp. 7581–7590, 2022c.

Feng Liang, Bichen Wu, Xiaoliang Dai, Kunpeng Li, Yinan Zhao, Hang Zhang, Peizhao Zhang, Peter Vajda, and Diana Marculescu. Open-vocabulary semantic segmentation with mask-adapted clip. In *Proceedings of the IEEE/CVF Conference on Computer Vision and Pattern Recognition*, pp. 7061–7070, 2023.

Mingsheng Long, Yue Cao, Jianmin Wang, and Michael Jordan. Learning transferable features with deep adaptation networks. In *International conference on machine learning*, pp. 97–105. PMLR, 2015.

Mingsheng Long, Zhangjie Cao, Jianmin Wang, and Michael I Jordan. Conditional adversarial domain adaptation. *Advances in neural information processing systems*, 31, 2018.

Neil Houlsby Matthias Minderer, Alexey Gritsenko. Scaling open-vocabulary object detection. *NeurIPS*, 2023.

Ke Mei, Chuang Zhu, Jiaqi Zou, and Shanghang Zhang. Instance adaptive self-training for unsupervised domain adaptation. In *Computer Vision–ECCV 2020: 16th European Conference, Glasgow, UK, August 23–28, 2020, Proceedings, Part XXVI 16*, pp. 415–430. Springer, 2020.

Gerhard Neuhold, Tobias Ollmann, Samuel Rota Bulo, and Peter Kontschieder. The mapillary vistas dataset for semantic understanding of street scenes. In *Proceedings of the IEEE international conference on computer vision*, pp. 4990–4999, 2017.

Yingwei Pan, Ting Yao, Yehao Li, Yu Wang, Chong-Wah Ngo, and Tao Mei. Transferrable prototypical networks for unsupervised domain adaptation. In *Proceedings of the IEEE/CVF conference on computer vision and pattern recognition*, pp. 2239–2247, 2019.

Sanqing Qu, Tianpei Zou, Lianghua He, Florian Röhrbein, Alois Knoll, Guang Chen, and Changjun Jiang. Lead: Learning decomposition for source-free universal domain adaptation. In *Proceedings of the IEEE/CVF Conference on Computer Vision and Pattern Recognition*, pp. 23334–23343, 2024.

Alec Radford, Jong Wook Kim, Chris Hallacy, Aditya Ramesh, Gabriel Goh, Sandhini Agarwal, Girish Sastry, Amanda Askell, Pamela Mishkin, Jack Clark, et al. Learning transferable visual models from natural language supervision. In *International conference on machine learning*, pp. 8748–8763. PMLR, 2021.

Tianhe Ren, Shilong Liu, Ailing Zeng, Jing Lin, Kunchang Li, He Cao, Jiayu Chen, Xinyu Huang, Yukang Chen, Feng Yan, et al. Grounded sam: Assembling open-world models for diverse visual tasks. *arXiv preprint arXiv:2401.14159*, 2024.

Stephan R Richter, Vibhav Vineet, Stefan Roth, and Vladlen Koltun. Playing for data: Ground truth from computer games. In *Computer Vision–ECCV 2016: 14th European Conference, Amsterdam, The Netherlands, October 11-14, 2016, Proceedings, Part II 14*, pp. 102–118. Springer, 2016.

Kuniaki Saito and Kate Saenko. Ovanet: One-vs-all network for universal domain adaptation. In *Proceedings of the ieee/cvf international conference on computer vision*, pp. 9000–9009, 2021.

Cheng Shi and Sibei Yang. The devil is in the object boundary: towards annotation-free instance segmentation using foundation models. *arXiv preprint arXiv:2404.11957*, 2024.

Lianghe Shi and Weiwei Liu. Adversarial self-training improves robustness and generalization for gradual domain adaptation. *Advances in Neural Information Processing Systems*, 36, 2024.

Remi Tachet des Combes, Han Zhao, Yu-Xiang Wang, and Geoffrey J Gordon. Domain adaptation with conditional distribution matching and generalized label shift. *Advances in Neural Information Processing Systems*, 33:19276–19289, 2020.

Song Tang, Wenxin Su, Mao Ye, and Xiatian Zhu. Source-free domain adaptation with frozen multimodal foundation model. In *Proceedings of the IEEE/CVF Conference on Computer Vision and Pattern Recognition*, pp. 23711–23720, 2024.

Hugo Touvron, Thibaut Lavril, Gautier Izacard, Xavier Martinet, Marie-Anne Lachaux, Timothée Lacroix, Baptiste Rozière, Naman Goyal, Eric Hambro, Faisal Azhar, et al. Llama: Open and efficient foundation language models. *arXiv preprint arXiv:2302.13971*, 2023.

Yi-Hsuan Tsai, Wei-Chih Hung, Samuel Schulter, Kihyuk Sohn, Ming-Hsuan Yang, and Manmohan Chandraker. Learning to adapt structured output space for semantic segmentation. In *Proceedings of the IEEE conference on computer vision and pattern recognition*, pp. 7472–7481, 2018.

Girish Varma, Anbumani Subramanian, Anoop Namboodiri, Manmohan Chandraker, and CV Jawahar. Idd: A dataset for exploring problems of autonomous navigation in unconstrained environments. In *2019 IEEE winter conference on applications of computer vision (WACV)*, pp. 1743–1751. IEEE, 2019.

Feng Wang, Jieru Mei, and Alan Yuille. Sclip: Rethinking self-attention for dense vision-language inference. *arXiv preprint arXiv:2312.01597*, 2023.

Zhixiang Wei, Lin Chen, Yi Jin, Xiaoxiao Ma, Tianle Liu, Pengyang Ling, Ben Wang, Huaian Chen, and Jinjin Zheng. Stronger fewer & superior: Harnessing vision foundation models for domain generalized semantic segmentation. In *Proceedings of the IEEE/CVF Conference on Computer Vision and Pattern Recognition*, pp. 28619–28630, 2024.

Thomas Westfechtel, Hao-Wei Yeh, Qier Meng, Yusuke Mukuta, and Tatsuya Harada. Backprop induced feature weighting for adversarial domain adaptation with iterative label distribution alignment. In *Proceedings of the IEEE/CVF winter conference on applications of computer vision*, pp. 392–401, 2023.

Jianzong Wu, Xiangtai Li, Henghui Ding, Xia Li, Guangliang Cheng, Yunhai Tong, and Chen Change Loy. Betrayed by captions: Joint caption grounding and generation for open vocabulary instance segmentation. In *Proceedings of the IEEE/CVF International Conference on Computer Vision*, pp. 21938–21948, 2023a.

Size Wu, Wenwei Zhang, Lumin Xu, Sheng Jin, Xiangtai Li, Wentao Liu, and Chen Change Loy. Clipself: Vision transformer distills itself for open-vocabulary dense prediction. *arXiv preprint arXiv:2310.01403*, 2023b.

Yongqin Xian, Subhabrata Choudhury, Yang He, Bernt Schiele, and Zeynep Akata. Semantic projection network for zero-and few-label semantic segmentation. In *Proceedings of the IEEE/CVF Conference on Computer Vision and Pattern Recognition*, pp. 8256–8265, 2019.

Enze Xie, Wenhai Wang, Zhiding Yu, Anima Anandkumar, Jose M Alvarez, and Ping Luo. Segformer: Simple and efficient design for semantic segmentation with transformers. *Advances in neural information processing systems*, 34:12077–12090, 2021.

Gonca Yilmaz, Songyou Peng, Francis Engelmann, Marc Pollefeys, and Hermann Blum. Opendas: Domain adaptation for open-vocabulary segmentation. *arXiv preprint arXiv:2405.20141*, 2024.

Kaichao You, Mingsheng Long, Zhangjie Cao, Jianmin Wang, and Michael I Jordan. Universal domain adaptation. In *Proceedings of the IEEE/CVF conference on computer vision and pattern recognition*, pp. 2720–2729, 2019.

Qihang Yu, Ju He, Xueqing Deng, Xiaohui Shen, and Liang-Chieh Chen. Convolutions die hard: Open-vocabulary segmentation with single frozen convolutional clip. *Advances in Neural Information Processing Systems*, 36, 2024.

Haobo Yuan, Xiangtai Li, Chong Zhou, Yining Li, Kai Chen, and Chen Change Loy. Open-vocabulary sam: Segment and recognize twenty-thousand classes interactively. *arXiv preprint arXiv:2401.02955*, 2024.

Giacomo Zara, Subhankar Roy, Paolo Rota, and Elisa Ricci. Autolabel: Clip-based framework for open-set video domain adaptation. In *Proceedings of the IEEE/CVF Conference on Computer Vision and Pattern Recognition*, pp. 11504–11513, 2023.

C Zhang, D Han, Y Qiao, JU Kim, SH Bae, S Lee, and CS Hong. Faster segment anything: Towards lightweight sam for mobile applications. arxiv 2023. *arXiv preprint arXiv:2306.14289*.

Pan Zhang, Bo Zhang, Ting Zhang, Dong Chen, Yong Wang, and Fang Wen. Prototypical pseudo label denoising and target structure learning for domain adaptive semantic segmentation. In *Proceedings of the IEEE/CVF conference on computer vision and pattern recognition*, pp. 12414–12424, 2021.

Yixin Zhang, Zilei Wang, Junjie Li, Jiafan Zhuang, and Zihan Lin. Towards effective instance discrimination contrastive loss for unsupervised domain adaptation. In *Proceedings of the IEEE/CVF International Conference on Computer Vision*, pp. 11388–11399, 2023.

Jingxing Zhou and Jürgen Beyerer. Category differences matter: A broad analysis of inter-category error in semantic segmentation. In *Proceedings of the IEEE/CVF Conference on Computer Vision and Pattern Recognition (CVPR) Workshops*, pp. 3870–3880, June 2023.

A APPENDIX

OVERVIEW

The supplementary material presents the following sections to strengthen the main manuscript:

- **Sec. A.1** includes more implementation details.
- **Sec. A.2** presents memory usage and computational efficiency comparison.
- **Sec. A.3** provides examples and further explanation of naive combination of HRDA with open-vocabulary approaches, as mentioned in Table 1
- **Sec. A.4** presents ablations on CLIP confidence thresholding.
- **Sec. A.5** provides additional experimental results under different DA settings.
- **Sec. A.6** provides detailed per-class experimental results in Table 1.
- **Sec. A.7 and Sec. A.8** provides details of building taxonomy mapping and context descriptions for each target label.

A.1 MODEL ARCHITECTURE AND TRAINING

HRDA for UDA segmentation model For the UDA segmentation model, we follow HRDA (Hoyer et al., 2022b). We follow the HRDA framework, which combines large low-resolution (LR) crops for capturing scene context with small high-resolution (HR) crops for fine detail. These two types of inputs are combined using a learned scale attention mechanism, which enables the model to effectively handle multi-resolution information. In addition, HRDA uses overlapping slide inference to refine the generated pseudo-labels, ensuring that the context and details of the images are well-represented in the segmentation maps. The HRDA framework builds on the DAFormer (Hoyer et al., 2022a) architecture, which incorporates a domain-robust transformer backbone to extract features and perform segmentation. A self-training strategy with a teacher-student model is used, where the teacher generates pseudo-labels for the target domain, and these pseudo-labels are weighted based on a confidence score to prevent error accumulation during training. The teacher model is updated using an exponential moving average (EMA) of the student model's weights, ensuring stable pseudo-labels over time. In our experiments, we follow the default training parameters in the GTA $\rightarrow$ CityScapes setting and adapt from the labeled GTA dataset to the unlabeled Mapillary Vistas/IDD respectively. The labeled GTA training set and unlabeled Mapillary Vistas/IDD training set are used to train the UDA Framework.

Mask2Former for target domain segmentation To train a domain-specific model on the target domain, we utilize the Mask2Former architecture. The model comprises a backbone network that extracts low-resolution features, a pixel decoder that upscales these features, and a transformer decoder for processing object queries. It deploys masked attention, which focuses on local regions of the predicted mask, improving convergence and handling small objects. In our experiment, we generate pseudo-labels on the target training set using DynAlign and train Mask2Former with these labels on the target dataset to improve segmentation performance.

All experiments are conducted on NVIDIA A100-SXM4-80GB GPU.

A.2 COMPUTATIONAL EFFICIENCY

Our method comprises three main components: the UDA semantic segmentation model (HRDA), SAM, and CLIP. For semantic segmentation on high-resolution images, the memory usage primarily depends on the semantic segmentation model (HRDA), while the inference time is influenced by the reassignment of novel class labels. We provide detailed information on memory usage, inference time, and model parameters in table 5.

The total model parameter count of our method includes the UDA model parameters, plus 308M for SAM (ViT-L) and 351M for CLIP (ConvNeXt-Large). The reported total memory usage corresponds to the memory allocated during the complete inference process for a single image. Overall, our

Table 5: Computational efficiency and memory usage of DynAlign

Model	Memory Usage	Inference Time	Model Parameters
HRDA	23.9 GB	1.9 s	86 M
Ours (HRDA)	34.8 GB	64.1 s	668 M
DAFormer	10.5 GB	0.7 s	86 M
Ours (DAFormer)	21.7 GB	64.1 s	668 M
Ours (pseudo-label, HRDA)	23.9 GB	1.9 s	86 M
Ours (pseudo-label, DAFormer)	10.5 GB	0.7 s	86 M
Ours (pseudo-label, Mask2Former)	3.7 GB	0.3 s	215 M

framework requires reasonable computational resources. Moreover, the UDA framework can be flexibly substituted to accommodate memory limitations. As shown in the table, replacing HRDA with DAFormer significantly reduces memory consumption. For efficient inference, a segmentation model can also be trained using pseudo-labels generated by our framework, as described in *Section 5.3*. For example, a trained Mask2Former model using our inference pseudo labels, indicated as Ours (pseudo-label, Mask2Former), achieves inference in just 0.3 seconds per single image, offering a significant efficiency boost while maintaining high performance.

A.3 Examples of naive combination of HRDA with open-vocabulary approaches

For a naive combination of in-domain predictions with prior knowledge as baseline methods, we take the in-domain segmentation results produced by HRDA and layer them with the new class predictions from open-vocabulary models. As demonstrated in Figure 6, the open-vocabulary predictions for known classes in the source domain label space are discarded. This ensures that only novel class predictions from the open-vocabulary model are added on top of the HRDA predictions, preserving in-domain knowledge from HRDA.

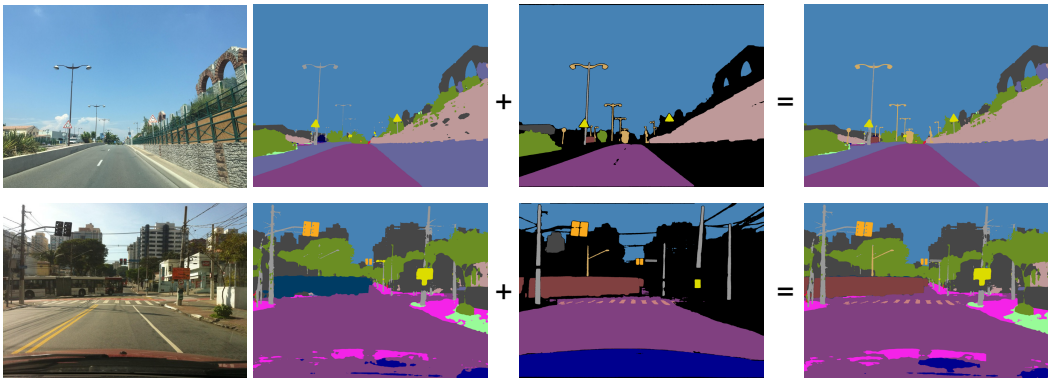

(a) Image (b) HRDA (c) Grounded-SAM (d) HRDA + Grounded-SAM

Figure 6: Illutration on HRDA+Grounded-SAM baseline

A.4 Ablations on CLIP confidence threshold

In our experiments, we set the confidence threshold to 0.5 by default for reassigning the class label. We conduct ablation studies with varying confidence thresholds, as presented in Table 6. The results show that while the mAcc improves with a lower confidence threshold for assigning new class labels, the mIoU may decrease correspondingly. Overall, DynAlign demonstrates robustness and is not very sensitive to the confidence threshold within a certain value range.

Table 6: Ablations on CLIP confidence threshold

Threshold	0.4	0.5	0.6	0.7	0.8	0.9
mIoU	35.9	36.7	37.6	36.5	36.6	36.5
mAcc	54.3	53.0	52.1	50.3	47.3	46.5

A.5 Experiments under more DA settings

To validate the effectiveness of our methods in diverse practical scenarios, we implement additional experiments under the following settings: 1) Traditional UDA Setting: In this case, the target label space is identical to the source label space. We adapt from GTA to Cityscapes, both using the same label space. 2) Fine-to-Coarse Setting: Here, the target domain labels are coarser than the source domain labels. For this, we adapt from Mapillary (45 classes) to Cityscapes (19 classes). As shown in Table 7, in both the traditional UDA and fine-to-coarse settings, where sufficient domain knowledge about the label space is available, our framework preserves the in-domain performance and provides slight improvements when adequate in-domain knowledge is already present.

In Table 8, we present results under taxonomy-adaptive domain adaptation with a smaller label-space domain gap. Specifically, we adapt from Synthia (16 classes) to Cityscapes (19 classes). These results highlight that our method not only maintains strong performance on known classes but also predicts effectively for unknown classes.

Table 7: Semantic segmentation comparison on Mapillary under traditional UDA and fine-to-coarse setting

Setting	mIoU	mAcc
GTA to Cityscapes (HRDA, 19 $\rightarrow$ 19)	74.9	82.0
GTA to Cityscapes (Ours, 19 $\rightarrow$ 19)	75.9	83.7
Mapillary to Cityscapes (Ours, 45 $\rightarrow$ 19)	70.4	81.5

Table 8: Semantic segmentation comparison on Mapillary under coarse-to-fine setting with small label domain gap

Settings	all classes		known classes		unknown classes	
	mIoU	mAcc	mIoU	mAcc	mIoU	mAcc
Synthia to Cityscapes (HRDA, 16 $\rightarrow$ 16)	N/A	N/A	66.8	73.7	N/A	N/A
Synthia to Cityscapes (Ours, 16 $\rightarrow$ 19)	61.6	72.7	68.8	77.5	23.2	47.0

A.6 Per-class evaluation results

For experimental results in Table 1, we provide the corresponding per-class evaluation in Table 9 and Table 10.

A.7 Taxonomy Mapping

We provide the detailed taxonomy mapping that maps each source label to its correlated target labels in Table 11 and Table 12. We utilizes GPT-4 to generate an initial proposal for potentially correlated taxonomy mappings between the source and target domains and introduce human intervention to refine these mappings due to the differing definitions of classes across datasets. For example, in the Mapillary dataset, the term "guard rail" specifically refers to roadside guard rails, whereas in other datasets or in general usage, it may represent a broader guarding fence. For the same reason, we exclude labels with inherent ambiguity, which we refer to classes that are broad or highly context-dependent. (For example, the class "other vehicles" may encompass various types of vehicles that are not explicitly defined in the dataset, making precise labeling a challenge. Similarly, the class "ego vehicle" refers specifically to the vehicle equipped with the camera, which often appears only partially in the image.) We examine the generated taxonomy mapping to ensure that the mappings

Table 9: Per-class semantic segmentation evaluation results on Mapillary. (lane marking is refered as lm).

	Grounded-SAM		Grounded-SAM + HRDA		OwlVIT-SAM		OwlVIT-SAM + HRDA		Ours	
	IoU	Acc	IoU	Acc	IoU	Acc	IoU	Acc	IoU	Acc
curb	1.6	1.6	1.6	1.6	18.7	27.0	18.7	27.0	16.3	44.9
fence	30.3	33.3	40.0	48.1	18.9	22.3	32.9	37.8	45.6	53.2
guard rail	21.3	28.8	21.3	28.8	17.9	36.1	17.9	36.1	15.3	21.1
wall	1.3	1.4	35.5	55.2	11.4	19.3	30.4	41.8	39.3	59.0
rail track	10.7	12.0	10.7	12.0	2.2	4.3	2.2	4.3	17.0	18.1
road	81.9	93.7	79.0	93.5	54.0	58.6	58.5	65.9	70.2	77.1
sidewalk	33.0	34.6	42.7	64.0	32.2	43.0	40.3	53.7	27.8	33.3
bridge	41.7	46.8	41.7	46.8	30.7	43.6	30.7	43.6	20.8	23.3
building	70.1	81.6	80.3	94.5	44.0	52.8	71.8	81.1	76.5	85.6
tunnel	0.0	0.0	0.0	0.0	1.2	3.6	1.2	3.6	13.4	79.5
person	67.9	78.6	74.9	85.6	29.5	33.3	69.0	78.3	77.7	89.3
bicyclist	8.3	9.4	21.6	36.4	10.6	12.6	35.1	66.8	53.8	72.0
motorcyclist	13.9	32.1	13.9	32.1	9.9	11.7	9.9	11.7	51.6	58.3
lm - crosswalk	20.3	24.4	20.3	24.4	8.9	14.8	8.9	14.8	20.0	56.6
lm - general	1.6	1.6	1.6	1.6	12.4	19.8	12.4	19.8	18.0	41.8
mountain	29.1	32.9	29.1	32.9	16.1	37.8	16.1	37.8	43.8	56.5
sand	29.6	35.7	29.6	35.7	24.1	38.1	24.1	38.1	18.4	49.2
sky	91.7	92.9	94.8	99.0	69.0	70.5	73.2	76.1	95.1	97.8
snow	34.1	34.5	34.1	34.5	26.9	38.9	26.9	38.9	40.9	77.5
terrain	12.3	12.5	48.1	93.1	0.3	0.3	47.6	82.7	48.5	84.4
vegetation	28.0	28.3	81.2	85.3	19.1	20.3	72.3	75.5	82.0	85.7
water	81.1	81.7	81.1	81.7	72.2	87.9	72.2	87.9	47.3	56.0
banner	5.3	5.4	5.3	5.4	6.8	10.0	6.8	10.0	0.5	0.7
bench	44.3	48.7	44.3	48.7	23.7	46.4	23.7	46.4	1.2	78.9
billboard	12.9	15.1	12.9	15.1	15.3	32.1	15.3	32.1	28.1	55.8
catch basin	0.0	0.0	0.0	0.0	0.0	0.0	0.0	0.0	8.9	18.1
manhole	19.3	19.8	19.3	19.8	20.4	40.5	20.4	40.5	23.7	25.3
phone booth	12.8	26.6	12.8	26.6	1.9	35.7	1.9	35.7	0.8	57.8
street light	8.0	46.4	8.0	46.4	3.0	32.6	3.0	32.6	15.2	21.2
pole	22.4	24.9	33.0	43.6	15.5	16.6	29.1	37.2	41.9	57.6
traffic sign frame	0.4	0.9	0.4	0.9	3.2	7.6	3.2	7.6	0.1	0.1
utility pole	27.0	31.1	27.0	31.1	23.2	29.5	23.2	29.5	23.8	25.2
traffic light	60.3	64.5	56.4	65.1	26.2	28.1	53.5	61.0	59.8	73.0
traffic sign (back)	0.0	0.0	0.0	0.0	7.8	19.9	7.8	19.9	3.4	5.1
traffic sign (front)	30.7	32.5	40.4	43.1	29.2	32.0	45.8	48.1	61.8	66.8
trash can	48.5	49.8	48.5	49.8	28.0	42.9	28.0	42.9	15.0	19.4
bicycle	57.1	63.6	49.9	54.3	28.1	58.1	49.0	53.3	57.1	62.9
boat	40.0	62.9	40.0	62.9	12.4	63.8	12.4	63.8	7.4	12.8
bus	76.0	81.7	60.9	67.1	39.7	60.6	51.8	56.7	68.3	73.1
car	62.1	64.5	65.1	68.1	26.9	34.6	49.6	51.7	88.1	92.0
caravan	0.0	0.0	0.0	0.0	0.0	0.2	0.0	0.2	24.1	82.6
motorcycle	49.2	52.8	53.2	61.4	37.2	39.7	54.9	62.9	65.1	76.6
on rails	0.0	0.0	9.0	10.2	0.0	0.0	28.1	30.4	53.3	59.3
trailer	0.0	0.0	0.0	0.0	0.1	5.7	0.1	5.7	1.4	20.0
truck	0.0	0.0	11.5	13.5	0.0	0.0	14.3	16.5	65.0	80.4
Average	28.6	33.1	32.9	40.4	19.5	29.6	28.8	40.2	36.7	53.0

are accurate and contextually appropriate. The taxonomy mapping significantly reduces effort compared to tasks such as pixel-wise manual annotation and only needs to be defined once per dataset pair. We highlight the identical classes in source and target domains in blue.

A.8 Context Names

We provide the context names used to describe the target names under the scene context in Table 13, 14, and 15. We generate those names by providing GPT-4 with the instruction:

Table 10: Per-class semantic segmentation evaluation results on IDD

	Grounded-SAM		Grounded-SAM + HRDA		OwlVIT-SAM		OwlVIT-SAM + HRDA		Ours	
	IoU	Acc	IoU	Acc	IoU	Acc	IoU	Acc	IoU	Acc
road	83.5	88.9	84.6	94.5	76.0	81.9	84.9	96.4	85.9	99.1
drivable fallback	17.2	23.9	17.2	23.9	0.0	0.0	0.0	0.0	2.9	3.4
sidewalk	15.8	18.8	12.8	68.9	3.6	17.7	15.6	74.6	17.0	72.2
non-drivable fallback	13.8	18.8	13.7	14.2	1.9	2.4	14.1	14.6	4.9	5.1
person	25.1	71.8	57.3	72.7	13.6	27.4	56.8	71.8	59.5	74.6
rider	0.2	0.2	64.4	78.4	0.6	0.6	63.5	77.2	67.7	80.3
motorcycle	57.4	62.9	64.4	77.4	34.2	36.4	64.1	77.0	67.2	80.1
bicycle	33.7	36.2	15.2	38.5	2.6	34.0	16.2	38.4	15.8	39.5
autorickshaw	0.0	0.0	0.0	0.0	34.7	46.0	34.7	46.0	36.5	81.4
car	84.5	88.9	63.8	96.8	22.8	23.1	69.0	96.0	70.2	80.9
truck	72.3	77.8	86.2	91.7	31.6	35.2	80.7	84.9	86.8	91.9
bus	74.8	81.6	68.4	71.4	42.8	47.8	63.6	66.1	68.8	71.9
curb	6.8	7.3	6.8	7.3	14.9	30.6	14.9	30.6	14.7	18.2
wall	4.7	4.7	40.8	66.5	8.0	8.9	40.8	59.8	41.9	67.6
fence	8.3	21.2	20.2	33.8	5.5	13.4	21.5	34.9	22.3	35.1
guard rail	8.2	13.0	8.2	13.0	9.3	28.5	9.3	28.5	13.9	22.1
billboard	22.3	23.7	22.3	23.7	16.1	25.8	16.1	25.8	43.9	60.7
traffic sign	14.8	16.0	10.3	33.1	16.3	70.4	23.3	78.2	31.0	80.3
traffic light	23.7	24.5	19.5	22.5	6.4	13.1	19.3	22.3	23.9	27.2
pole	8.7	8.8	34.1	39.4	19.2	21.5	33.8	38.9	35.4	41.0
obs-str-bar-fallback	0.9	0.9	0.9	0.9	0.0	0.0	0.0	0.0	6.4	9.5
building	45.3	60.0	51.8	87.1	26.1	49.0	52.0	83.9	54.3	82.6
bridge	43.3	44.2	43.3	44.2	31.6	60.4	31.6	60.4	8.1	44.7
vegetation	12.4	12.4	84.5	94.5	21.5	22.6	84.3	94.0	80.6	87.0
sky	91.4	92.8	94.6	98.8	84.1	93.8	94.7	98.7	82.3	85.3
Average	30.8	36.0	39.4	51.7	20.9	31.6	40.2	55.9	41.7	57.7

Table 11: Taxonomy mapping from GTA to Mapillary

Source Label	Target Label Set
road	road, sidewalk, snow, sand, water, catch basin, manhole, rail track, lane marking-crosswalk, lane marking-general
sidewalk	sidewalk, curb, snow, sand, water
building	building, bridge, tunnel, phone booth, billboard,
wall	wall, bridge, tunnel, trash can, banner, billboard
fence	fence, guard rail
pole	pole, utility pole, trash can, banner, street light, traffic sign frame
traffic light	traffic light, street light
traffic sign	traffic sign (front), traffic sign (back), billboard, banner
vegetation	vegetation, snow
terrain	terrain, mountain, snow, sand, water
sky	sky
person	person
rider	bicyclist, motorcyclist
car	car, trailer, boat
truck	truck, caravan
bus	bus
train	on rails
motorcycle	motorcycle
bicycle	bicycle
unlabeled	bench, billboard, bridge, tunnel

Generate new class names within the context of street scene semantic segmentation, using the original class name as the head noun. Use synonyms or subcategories of the original class that make sense within this context, and if the class has multiple meanings, add specific context to avoid ambiguity. Please provide the original class names along with context names.

Table 12: Taxonomy mapping from GTA to IDD

Source Label	Target Label Set
road	road, sidewalk, drivable fallback
sidewalk	sidewalk, curb, drivable fallback, non-drivable fallback
building	building, bridge, billboard,
wall	wall, obs-str-bar-fallback, bridge, billboard
fence	fence, guard rail, obs-str-bar-fallback
pole	pole
traffic light	traffic light
traffic sign	traffic sign, billboard, banner
vegetation	vegetation, obs-str-bar-fallback
terrain	terrain, non-drivable fallback, obs-str-bar-fallback
sky	sky
person	person
rider	bicyclist, motorcyclist
car	car, autorickshaw
truck	truck, caravan
bus	bus
train	other vehicles
motorcycle	motorcycle
bicycle	bicycle
unlabeled	billboard, bridge

For each label, we generate 10 context names. For labels without ambiguity, e.g. sky, we only use the original label for the text feature extraction.

Table 13: Context names for IDD labels

Target Label	**Context Names**
road	road, main road, driving lane, paved road, highway, residential street, arterial road, rural road, city road, thoroughfare
drivable fallback	drivable terrain, traffic lane, vehicle lane, driveable path, car lane, driveable street, urban roadway, paved path, driveable surface, roadway
sidewalk	sidewalk, pavement, footpath, walkway, pedestrian path, side path, sidewalk pavement, urban sidewalk, street sidewalk, sidewalk lane, sidewalk area
non-drivable fallback	non-drivable terrain, pedestrian area, park path, garden path, bike lane, footpath, public plaza, grass area, green space, pedestrian walkway, non-driveable zone
person	person
rider	rider
motorcycle	motorcycle
bicycle	bicycle
autorickshaw	autorickshaw, three-wheeler, tuk-tuk, auto-rickshaw, motorized rickshaw, auto taxi, rickshaw, three-wheeled taxi, auto, motor tricycle, auto rickshaw
car	car, sedan, hatchback, coupe, convertible, SUV, sports car, station wagon, compact car, electric car, luxury car
truck	truck, pickup truck, semi-truck, delivery truck, dump truck, fire truck, tow truck, box truck, flatbed truck, garbage truck, tanker truck
bus	bus
vehicle fallback	other vehicles, train, tram, metro, trolleybus, light rail, cable car
curb	curb, road curb, sidewalk curb, curbside, street curb, pavement curb, curb edge, curb line, curb boundary, urban curb, curb strip
wall	wall, barrier wall, protective wall, retaining wall, boundary wall, perimeter wall, dividing wall, sound barrier wall, security wall, freestanding wall, partition wall
fence	fence, building fence, road fence, vehicle separation fence, pedestrian fence, safety fence, boundary fence, traffic fence, divider fence, protective fence, barrier fence
guard rail	guard rail, road guard rail, highway guard rail, safety guard rail, traffic guard rail, barrier guard rail, roadside guard rail, protective guard rail, metal guard rail, crash barrier, median guard rail
billboard	billboard, advertising billboard, roadside billboard, digital billboard, outdoor billboard, highway billboard, commercial billboard, urban billboard, street billboard, electronic billboard, large billboard
traffic sign	traffic sign, road sign, highway sign, street sign, regulatory sign, warning sign, directional sign, informational sign, traffic control sign, signpost, traffic marker
traffic light	traffic light, traffic signal, stoplight, traffic control light, intersection signal, traffic lamp, signal light, road signal, street light, traffic signal light, traffic control signal
pole	pole, street pole, lamp pole, traffic pole, sign pole, light pole, support pole, signal pole, flag pole, decorative pole, banner pole
obs-str-bar-fallback	obstructive structures and barriers, construction barrier, roadblock, traffic cone, temporary fence, safety barrier, barricade, obstruction, traffic barricade, road barrier, construction zone marker
building	building, structure, edifice, construction, residential building, commercial building, office building, apartment building, skyscraper, public building, urban building
bridge	road bridge, footbridge, pedestrian bridge, walking bridge, footpath bridge, foot crossing, small bridge, pedestrian crossing, walkway bridge, urban footbridge, trail bridge
vegetation	vegetation, urban vegetation, city greenery, roadside plants, street vegetation, urban foliage, city flora, park vegetation, public greenery, urban plants, green space
sky	sky

Table 14: Context names for Mapillary labels (Part 1)

Target Label	**Context Names**
Road	road, main road, driving lane, paved road, highway, residential street, arterial road, rural road, city road, thoroughfare
Snow	snow, snow pile, street snow, roadside snow, accumulated snow, snowbank, plowed snow, urban snow, compacted snow, snow drift, snow on pavement
Sand	sand, sand pile, street sand, roadside sand, piled sand, sandbank, accumulated sand, urban sand, sand on pavement, construction sand, loose sand
Catch Basin	catch basin, road catch basin, street catch basin, roadside catch basin, storm drain, drainage basin, sewer catch basin, street drain, gutter catch basin, road drain, stormwater basin
Manhole	manhole, road manhole, street manhole, sewer manhole, manhole cover, utility manhole, drainage manhole, storm drain manhole, roadside manhole, underground access, inspection manhole
Pothole	pothole, road pothole, street pothole, asphalt pothole, pavement pothole, highway pothole, surface pothole, pothole damage, roadway pothole, pothole crater, pothole on pavement
Bike Lane	bike lane, marked bike lane, roadside bike lane, main road bike lane, dedicated bike lane, paved bike lane, urban bike lane, bike path, protected bike lane, street bike lane, lane-marked bike lane
Rail Track	rail track, tram rail track, train rail track, street rail track, road rail track, urban rail track, tramway track, railroad track, commuter rail track, embedded rail track, rail track on pavement
Lane Marking - Crosswalk	crosswalk lane marking, street crosswalk marking, pedestrian crosswalk marking, zebra crossing marking, road crosswalk marking, intersection crosswalk marking, painted crosswalk, crosswalk lines, crosswalk road marking, sidewalk crosswalk marking
Lane Marking - General	general lane marking, road lane marking, street lane marking, highway lane marking, pavement lane marking, lane divider marking, traffic lane marking, lane line marking, roadway lane marking, lane boundary marking, asphalt lane marking
Water	water, urban water, river water, lake water, city river, roadside pond, street water, urban pond, city lake, small urban river, stormwater
Sidewalk	sidewalk, pavement, footpath, walkway, pedestrian path, side path, sidewalk pavement, urban sidewalk, street sidewalk, sidewalk lane, sidewalk area
Curb	curb, road curb, sidewalk curb, curbside, street curb, pavement curb, curb edge, curb line, curb boundary, urban curb, curb strip
Pedestrian Area	pedestrian area, street pedestrian area, pedestrian zone, pedestrian walkway, pedestrian street, urban pedestrian area, pedestrian plaza, pedestrian path, sidewalk pedestrian area, pedestrian crossing area, designated pedestrian area
Building	building, structure, edifice, construction, residential building, commercial building, office building, apartment building, skyscraper, public building, urban building
Bridge	road bridge, footbridge, pedestrian bridge, walking bridge, footpath bridge, foot crossing, small bridge, pedestrian crossing, walkway bridge, urban footbridge, trail bridge
Billboard	billboard, advertising billboard, roadside billboard, digital billboard, outdoor billboard, highway billboard, commercial billboard, urban billboard, street billboard, electronic billboard, large billboard
Tunnel	tunnel, road tunnel, tunnel entrance, highway tunnel, urban tunnel, vehicle tunnel, tunnel passage, tunnel opening, subway tunnel, underground tunnel, traffic tunnel
Wall	wall, barrier wall, protective wall, retaining wall, boundary wall, perimeter wall, dividing wall, sound barrier wall, security wall, freestanding wall, partition wall
Traffic Sign Frame	traffic sign frame, signpost frame, traffic sign holder, sign frame, sign support frame, road sign frame, traffic sign structure, sign mounting frame, sign frame support, traffic sign bracket
Trash Can	trash can, street trash can, public trash can, roadside trash can, outdoor trash can, urban trash can, sidewalk trash can, street garbage can, public waste bin, street litter bin, municipal trash can
Banner	banner, advertising banner, promotional banner, street banner, event banner, hanging banner, outdoor banner, banner sign, vertical banner, display banner, publicity banner
Fence	fence, building fence, road fence, vehicle separation fence, pedestrian fence, safety fence, boundary fence, traffic fence, divider fence, protective fence, barrier fence
Guard Rail	guard rail, road guard rail, highway guard rail, safety guard rail, traffic guard rail, barrier guard rail, roadside guard rail, protective guard rail, metal guard rail, crash barrier, median guard rail
Pole	pole, street pole, lamp pole, traffic pole, sign pole, light pole, support pole, signal pole, flag pole, decorative pole, banner pole
Utility Pole	utility pole, electric pole, telephone pole, power pole, transmission pole, cable pole, utility line pole, utility post, service pole, communication pole, distribution pole
Street Light	street light, street lamp, road light, streetlight, lamp post, street lighting, urban street light, sidewalk light, public street light, street lantern, street illumination
Front Side Of Traffic Sign	front side of traffic sign, traffic sign front, front face of traffic sign, sign front, traffic sign face, front panel of traffic sign, signboard front, traffic sign display, front view of traffic sign, sign front side, traffic sign surface
Back Side Of Traffic Sign	back side of traffic sign, traffic sign back, back face of traffic sign, sign back, rear of traffic sign, signboard back, traffic sign reverse, sign back panel, back side of sign, traffic sign rear view, reverse side of traffic sign
Traffic Light	traffic light, traffic signal, stoplight, traffic control light, intersection signal, traffic lamp, signal light, road signal, street light, traffic signal light, traffic control signal
Vegetation	vegetation, urban vegetation, city greenery, street vegetation, roadside vegetation, urban plants, city foliage, urban flora, street greenery, public vegetation, cityscape vegetation

Table 15: Context names for Mapillary labels (Part 2)

Target Label	**Context Names**
Terrain	terrain, urban terrain, city landscape, street terrain, roadside terrain, urban ground, cityscape terrain, urban land, urban surface, city terrain, urban topography
Mountain	mountain, mountain peak, mountain range, mountain slope, rocky mountain, highland mountain, mountain summit, alpine mountain, mountain ridge, forest mountain, mountain terrain
Sky	sky
Person	person
Bicyclist	bicyclist, bike rider, cyclist, bicycle rider, bicycle commuter, mountain biker, road cyclist
Motorcyclist	motorcyclist, motorcycle rider, motorcycle driver, motorbike rider, motorcycle commuter, road motorcyclist
Car	car, sedan, hatchback, coupe, convertible, SUV, sports car, station wagon, compact car, electric car, luxury car
Trailer	trailer, utility trailer, travel trailer, cargo trailer, flatbed trailer, camper trailer, enclosed trailer, livestock trailer, dump trailer
Boat	boat, sailboat, motorboat, fishing boat, speedboat, yacht, canoe, kayak, pontoon boat, dinghy, houseboat
Truck	truck, pickup truck, semi-truck, delivery truck, dump truck, fire truck, tow truck, box truck, flatbed truck, garbage truck, tanker truck
Caravan	caravan, travel caravan, camper caravan, motorhome, touring caravan, RV (recreational vehicle), fifth-wheel caravan, pop-up caravan, teardrop caravan, static caravan, off-road caravan
Bus	bus
On Rails	on rails
Motorcycle	motorcycle
Bicycle	bicycle
Bench	bench, street bench, public bench, park bench, sidewalk bench, outdoor bench, urban bench, pavement bench, city bench, public seating bench, roadside bench